Journal of Alloys and Compounds 689 (2016) 225–232

Contents lists available at ScienceDirect

Journal of Alloys and Compounds

journal homepage: http://www.elsevier.com/locate/jalcom

Effect of tempering temperature on microstructure and mechanical properties of laser solid formed 300M steel

Fenggang Liu, Xin Lin*, Menghua Song, Haiou Yang, Kan Song, Pengfei Guo, Weidong Huang

State Key Laboratory of Solidification Processing, Northwestern Polytechnical University, Xi'an 710072, PR China

ARTICLE INFO

Article history:
Received 17 February 2016
Received in revised form
19 July 2016
Accepted 26 July 2016
Available online 30 July 2016

Keywords:
Laser solid forming
Additive manufacturing
300M steel
Tempering temperature
Microstructure
Mechanical properties

ABSTRACT

The microstructure and mechanical properties of laser solid formed (LSFed) 300M steel with tempering treatment was investigated. The microstructure of laser solid formed 300M steel with tempering treatment mainly consisted of the tempered martensite, bainite and a small amount of retained austenite. When the tempering temperature increased from 250 °C to 350 °C, the size of martensite lath and martensite blocks changed little. There are two kinds of tempered martensite. With increase of the tempering temperature, ε-carbide in the general tempered martensite transformed to cementite. In another kind of tempered martensite, ε-carbide were found to be precipitated along specific growth directions, with at least two variants for carbide precipitation. The hardness presented an incomplete linear correlation with the tensile strength and the yield strength for LSFed 300M steel. The hardness in LSFed 300M steel had not shown a significant change with increase of the tempering temperature. The tensile strength and yield strength increased first till the tempering temperature reaches 290 °C–310 °C then decreased with further increasing the tempering temperature. Especially, the strength dramatically decreased when the tempering temperature was above 310 °C. However, the elongation and percentage reduction of area changed little with increase of the tempering temperature. The tensile fracture of LSFed 300M steel with tempering treatment presented a ductile fracture pattern.

1. Introduction

300M steel belongs to medium carbon low alloy steels. Due to its excellent tensile strength, fracture toughness and fatigue resistance, 300M steel has been widely used in landing gear, central spindle, wheel gear and so on [1–3]. As the major supporting component of the landing gear, 300M steel components are usually fabricated by die forging. However, it is difficult to manufacture the 300M steel components with a large scale and complex geometry by the die forge processing due to its high resistance of deformation. Recently, laser solid forming (LSF) of bulk near-net-shape metallic components using the additive manufacturing route has been shown to be a viable and promising manufacturing technology for building a large scale complex 300M steel components. LSF is an advanced laser additive manufacturing technology, which has been developed to fabricate metal parts with full density, any geometries and high performance [4]. In recent decades, with rapid development of LSF, more and more focuses have been used to fabricate the components [5–11].

To date, only a few works [12,13] focused on the LSFed 300M steel. Dong cui [12] studied the microstructure and hardness evolution along the deposition direction of as-deposited 300M steel. Liu [13] investigated that the tensile properties of LSFed 300M steel is significantly improved compared with the as-deposited after heat treatment. However, the research on the effects of the post heat treatment on the phase transformation and the mechanical properties of LSFed 300M steel is still lack, which is indispensable to the optimization of the mechanical properties of LSFed 300M steel components. Till now, the relevant studies were mainly focuses on the microstructure and mechanical properties of the forged 300M steel. The microstructure of quenched and tempered 300M steel forgings mainly consisted of the mixture of martensite, bainite and retained austenite, which plays a decisive role in the final mechanical properties. The previous research indicate that the width of martensite lath increases with the tempering temperature [14]. Conversely, the amount of retained austenite [15], dislocation

* Corresponding author.
E-mail address: xlin@nwpu.edu.cn (X. Lin).

http://dx.doi.org/10.1016/j.jallcom.2016.07.276
0925-8388/

density [16], strength and toughness are on the contrary. In addition, Youngblood [17] and Lee [18] found that the strength and toughness of low alloy ultrahigh strength steel is also obviously affected by the precipitation of finely dispersed carbides during tempering. They showed that the types and shapes of the carbides are related to the tempering condition. When the tempering temperature increases from 477 K to 700 K, the content of ε-carbide in the martensite gradually increases, the strength and toughness of the ultrahigh strength improves. However, when tempering at 700 K or above, the ε-carbide is transformed into cementite, the strength and toughness decrease [17]. Some researcher also studied the orientation relationship between the ε-carbide and the matrix [19–22]. They found that the orientation relationship of ferrite/austenite and ferrite/ε-carbide presented K-S relationship [20] and Jack relationship [19,20] respectively.

Based on the previous researches mentioned above on the forged 300M steel, it can be concluded that the morphology and the content of the composition phases of 300M steel depend on the heat treatment schedule, and also significantly affect the final mechanical properties. Furthermore, the tempering treatment can eliminate the residual stress and obtain the good comprehensive performances for 300M steel. Therefore, the systematic study on the microstructure evolution and the mechanical properties of the tempered LSFed 300M steel is highly desired. The process characterization of the LSF is remarkably different from the traditional cast and wrought, especially the existence of repeated incomplete rapid reheating annealing or tempering cycle in processing. In general, the LSFed parts possess several distinctive structure and mechanical features including large residual stress, fine microstructure and free of macro-segregation et al., which present a remarkable difference with the traditional as-cast and as-wrought. These features should lead to a significant influence on the final tempered microstructure of LSFed 300M steel. Thus, the main purpose of this paper includes: the microstructure evolution of martensite and bainite in LSFed 300M steel with different tempering temperature; the types and shapes of ε-carbides in the martensite; the effect of tempering temperature on the strength, plasticity, fracture morphology and micro-hardness.

2. Material and experimental procedures

The laser solid forming experiment was carried out in LSF-IIIB laser solid forming system, which consisted of 4 kW fast-axial-flow CO_2 laser, a five-axis numerical control working table, a powder feeding system with a coaxial nozzle. Pure argon was used as shielding gas, which was also used to carry alloy powders into the molten pool and to protect the molten pool from oxidation. 300M steel powder prepared by plasma rotating electrode processed (PREPed) and with the size of about 100–150 μm. The powder was dried in a vacuum oven for 4 h at 120 °C. The chemical composition of 300M steel powder was listed in Table 1. A 300M steel sheet was used as the substrate. The LSF processing parameters were listed as laser power 2800 W, spot diameter 3 mm, scanning rate 10 mm/s, overlapping ratio 45%, and single deposited height of 0.3–0.5 mm. A 300M steel block with the dimensions of 50 mm × 30 mm × 10 mm was built by LSF using the cross direction raster scanning path pattern. The block were tempered for 2 h, air cooling, two times. The tempering temperature is 250 °C, 270 °C, 290 °C, 310 °C, 330 °C, 350 °C, respectively. The heat-treatment regime of LSFed 300M steel was listed in Table 2.

Table 1
The chemical composition of 300M steel (wt%).

C	Si	Mn	S	P	Ni	Cr	Mo	V	Cu	Fe
0.38	1.45	0.60	≤	≤	1.65	0.70	0.30	0.05	≤	
~	~	~	0.01	0.01	~	~	~	~	0.35	Bal.
0.43	1.80	0.90			2.00	0.95	0.50	0.10		

For optical microscope microstructure observation, the samples were prepared through the standard metallographic practice. The microstructure of the samples with the tempering treatment were revealed using the etchant of 4% nital solution, and examined by OLYMPUS-GX71 optical microscope and TESCAN MIRA3 XMU field emission scanning electron microscopy (FE-SEM). Phase analysis was carried out with a TECNAI F30 G^2 transmission electron microscopy (TEM). Micro-hardness testing was conducted on an Struers Duramin-A300 Vickers microhardness tester with a load of 500 g and a dwell time of 15 s. Room temperature tensile properties of the heat-treated samples was carried out on an INSTRON 3382 tensile testing machine. Three samples were tested for each tempering case. The geometry of the tensile specimens was shown in Fig. 1. The tensile direction is perpendicular to the deposition direction.

3. Results and discussion

3.1. The microstructure evolution with the tempering temperature

Generally, the microstructure of quenched 300M steel is martensite, bainite and a small amount of retained austenite. The carbides will precipitate in martensite during low temperature tempering. The microstructure transforms to the tempered martensite. The microstructure of LSFed 300M steel tempered at the different temperature is shown in Fig. 2. The microstructure of the tempered LSFed 300M steel mainly consisted of tempered martensite, bainite and a small amount of retained austenite. There are several martensite blocks in the primary austenite grain. Each block contains a colony of martensite laths parallel to each other. The sheet-like bainite distributes among the martensite blocks as shown by the arrow in Fig. 2e. There is no obvious variation on the size of martensite blocks and laths with the tempering temperature. Actually, in previous researches [17,23–26], it is found that the size of the martensite has not significant changes in low alloy steels when the tempering temperature is below 700 K.

Table 2
Heat-treatment regime of laser solid formed 300M steel.

Sample	Quenching	Tempering
1	870 °C, 1 h/oil quenching	250 °C, 2 h/air cooling, two times
2	870 °C, 1 h/oil quenching	270 °C, 2 h/air cooling, two times
3	870 °C, 1 h/oil quenching	290 °C, 2 h/air cooling, two times
4	870 °C, 1 h/oil quenching	310 °C, 2 h/air cooling, two times
5	870 °C, 1 h/oil quenching	330 °C, 2 h/air cooling, two times
6	870 °C, 1 h/oil quenching	350 °C, 2 h/air cooling, two times

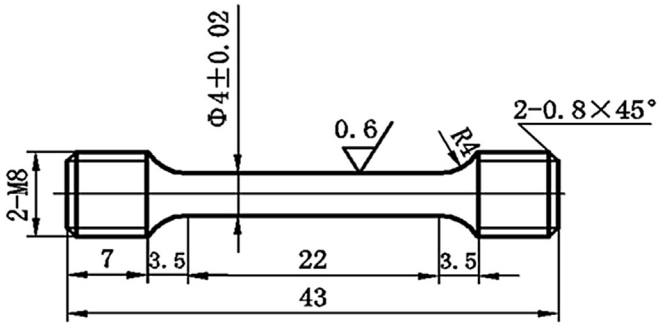

Fig. 1. Geometry of the tensile testing specimen (in mm).

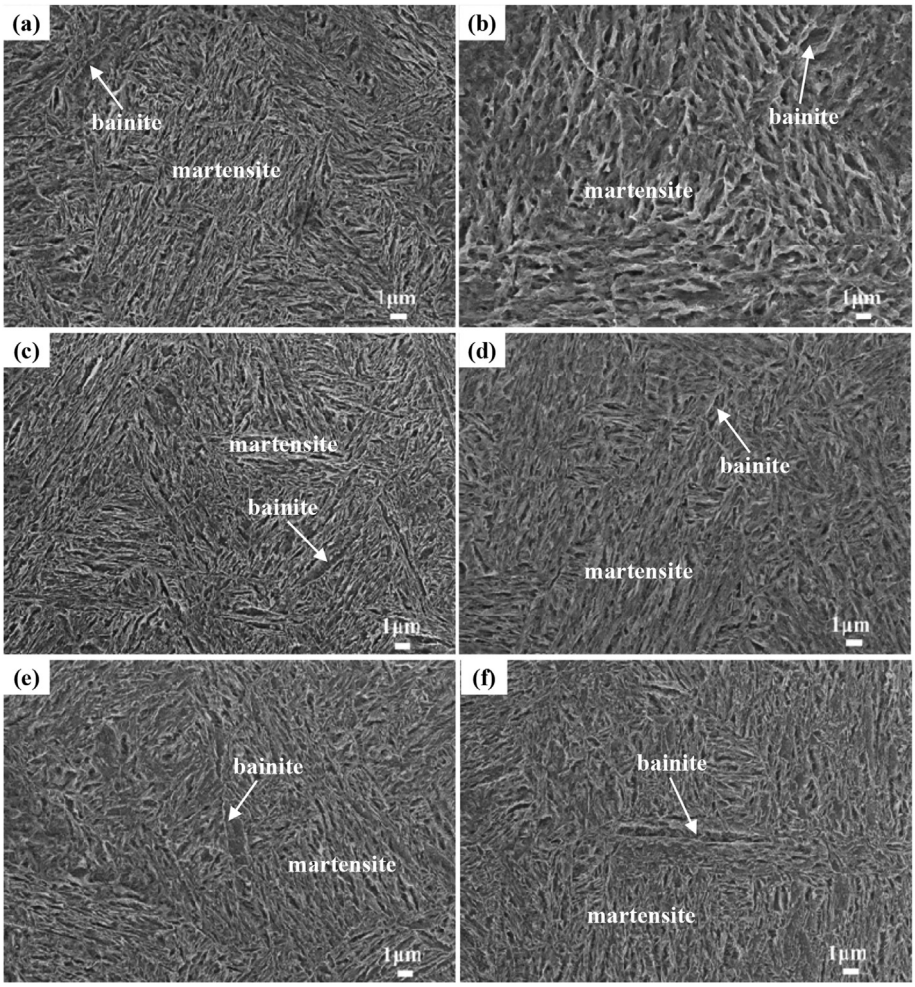

Fig. 2. The microstructure with different tempering temperature of laser solid formed 300M steel: (a) 250 °C, (b) 270 °C, (c) 290 °C, (d) 310 °C, (e) 330 °C, (f) 350 °C.

3.2. Phase transformations in the martensite

The phase transformations in the martensite with the different tempering temperature is shown in Fig. 3. With the increase of the tempering temperature, the phase transformations of the carbides in the martensite contains two stages:

1) The precipitated phase in the martensite is mainly ε-carbide when the tempering temperature is at 250 °C - 310 °C (Fig. 3c and f). The strip-like ε-carbide with a width of 20 nm and a length of 100–300 nm precipitates parallel to each other, which incline at an angle to the longitudinal axis of the lath boundary (Fig. 3a–b and d–e). The martensite will decompose during tempering and the ε-carbide precipitates from the parent martensite. The formation of the ε-carbide may be traced to the supersaturation of martensite with carbon leading to the generation of internal stresses, and lattice relaxation occurring via the precipitation of carbides. Jha, B.K [27]. studied the microstructural evolution during tempering of a multiphase steel and found that the severity of internal stresses is directly proportional to the carbon supersaruration. Simultaneously, the high internal stress is also a general characteristic in the LSFed samples. Thus promote the precipitation of the ε-carbide.
2) When the tempering temperature reaches 350 °C, the precipitated ε-carbide in the martensite transforms to cementite that is discontinuously arranged particles, as shown in Fig. 3g–h. As well known, the ε-carbide formed in the low tempering temperature is a metastable phase and tend to transform to the cementite. Generally, the transformation temperature of ε-carbide to cementite is about 260 °C in low alloy steel [26]. However, in this work, the transformation temperature is obviously raised (>310 °C at least) in 300M steel. Kozeschnik et al. [28] suggested that the reasons for the increase in ε-carbide transformation temperature can be attributed to the high silicon content (similar to the case of 300M steel, $wt\%_{si} = 1.6\%$). The silicon compositions in ε-carbide is comparable to that in the martensite. The cementite can be formed only when the ε-carbide is dissolved and released silicon atoms into the martensite. In the low tempering temperature, the mobility of the silicon element as the substitutional atom in the steel is limited, which retards the precipitation of cementite. Therefore, the phase transformation can only occur at elevated temperature in high-silicon steel.

In LSFed 300M steel, the precipitated carbide in the tempered martensite usually arranges in a single direction. But it is found that there exists another kind of tempered martensite, in which the carbide with the width of 20 nm and the length of 200 nm is precipitated in different directions, as shown in Fig. 4b and c. The selective area diffraction analysis of this carbide shows that it is also ε-carbide. The morphology of the ε-carbide in this tempered martensite might be related to the early behavior of the supersaturated carbon atoms in the quenched martensite. Carbon atoms can perform a short diffusion and then segregates at the defect sites within the period from the martensite start temperature to room

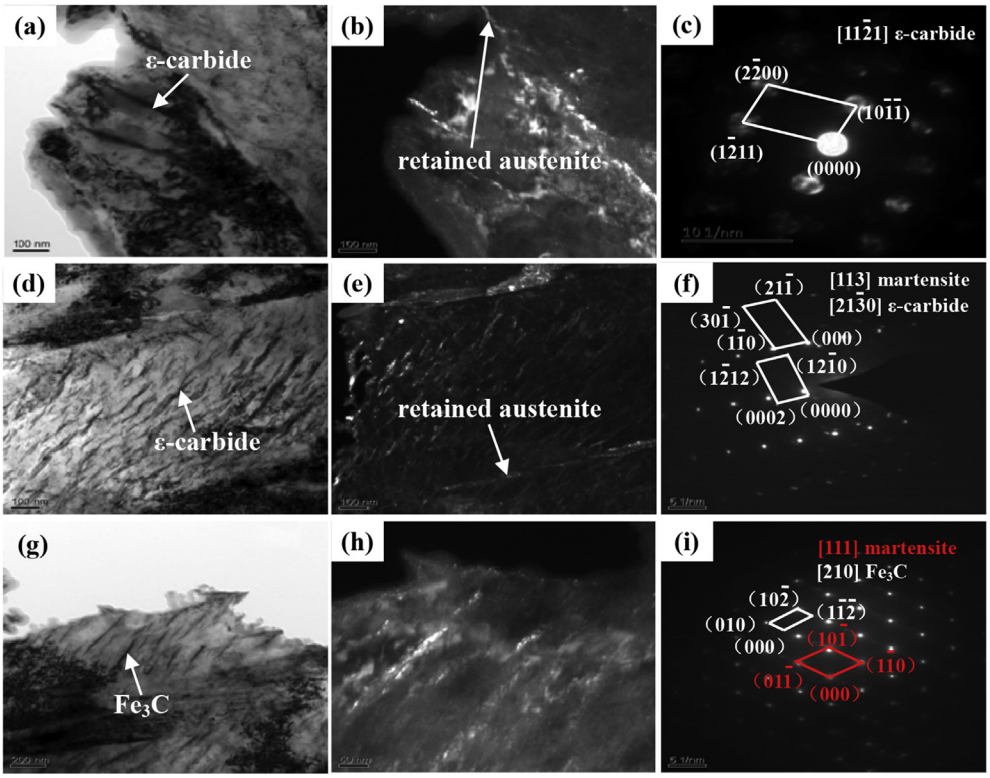

Fig. 3. The TEM images of phase in the martensite with different tempering temperature: (a) bright field of tempered martensite with tempered at 250 °C, (b) dark field of tempered martensite with tempered at 250 °C, (c) the selected area diffraction patterns of ε-carbide in the martensite with tempered at 250 °C, (d) bright field of tempered martensite with tempered at 310 °C, (e) dark field of tempered martensite with tempered at 310 °C, (f) the selected area diffraction patterns of ε-carbide in the martensite with tempered at 310 °C, (g) bright field of tempered martensite with tempered at 350 °C, (h) dark field of tempered martensite with tempered at 350 °C, (i) the selected area diffraction patterns of Fe_3C in the martensite with tempered at 350 °C.

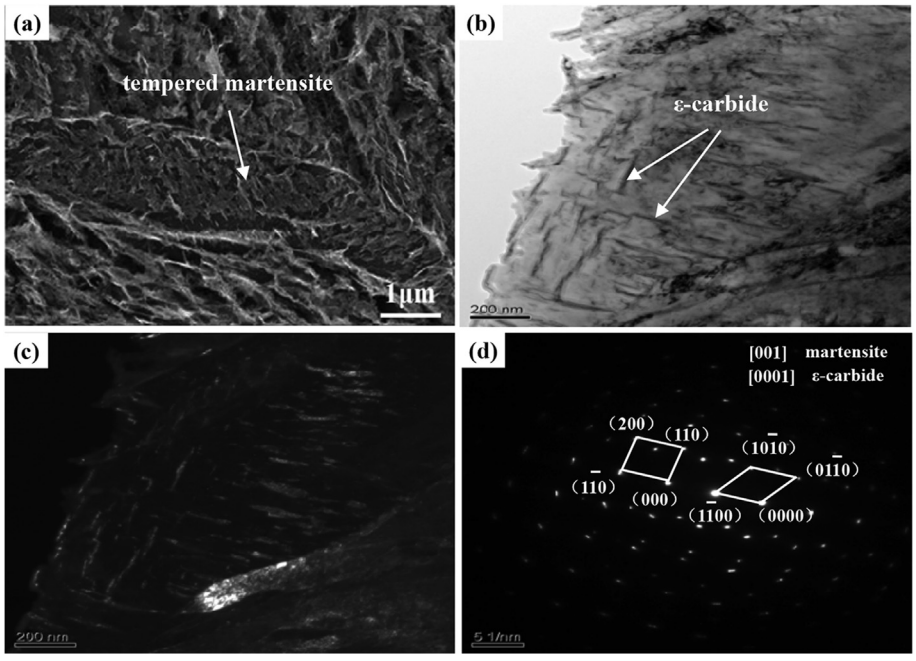

Fig. 4. The precipitated phase in the auto-tempered martensite: (a) SEM images of the precipitated phase, (b) bright field of precipitated phase, (c) dark field of precipitated phase, (d) the selective area diffraction pattern of precipitated phase.

temperature during the martensitic transformation [29,30]. Therefore, the dislocation patterns as the main defects of martensite have important effects on carbon segregation and the precipitation of the carbide. However, the dislocation patterns in the martensite mainly have four kinds of variants. But it is mainly two variants in each lath. So the precipitation of carbide might

appear the different directions.

3.3. The effect of microstructure on mechanical properties

The measured hardness on the tempered LSFed 300M steel are plotted in Fig. 5 as a function of the tempering temperature. The hardness gradually decreases with the increase of the tempering temperature and fluctuates in a small range of 600–650 H V. It can be seen from Fig. 6 that the tensile strength increases first and then decreases with the increase of the tempering temperature. It reaches the maximum (1966 MPa) with tempering at 290 °C. The yield strength has the similar trends with the increase of the tempering temperature and its maximum value is 1661 MPa when being tempered at 310 °C. Then, the yield strength sharply decrease to 1495 MPa when the tempering temperature reaches 350 °C. With the increase of the tempering temperature, the elongation and the percentage reduction of area have no obvious changes.

The microstructure of the tempered LSFed 300M steel mainly consists of the tempered martensite, bainite and a small amount of retained austenite. With the increase of the tempering temperature, the ε-carbide and the cementite gradually precipitate from the martensite. The supersaturation of the martensite decreases. And the solid solution strengthening of the carbon on the martensite reduces. The internal stress will be released. So the hardness

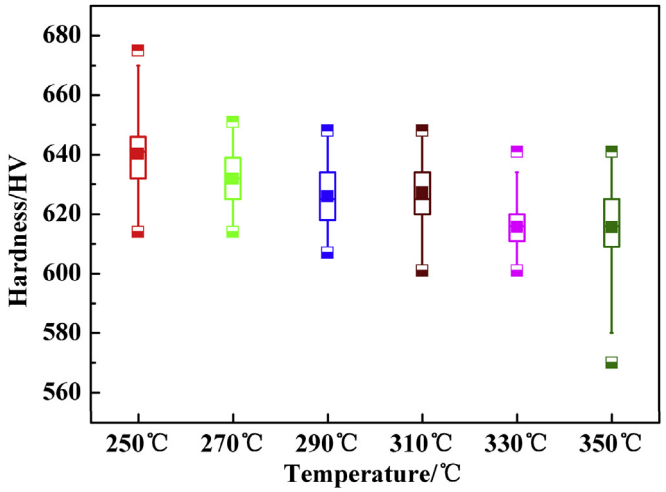

Fig. 5. The hardness curves with different tempering temperature of laser solid formed 300M steel.

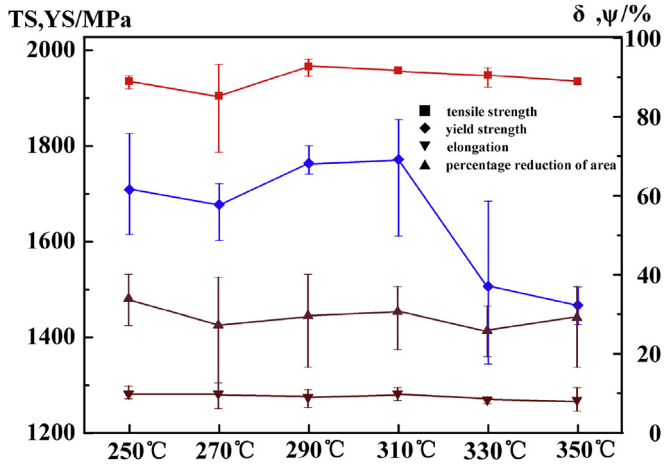

Fig. 6. The room temperature tensile strength of laser solid formed 300M steel with different tempering temperature.

gradually decreases. However, the size of the martensite blocks, martensite laths and bainite has no significant change with the increase of the tempering temperature. The hardness of the ε-carbide and the cementite is higher than that of the matrix. As a result of the combination of the two factors mentioned above, the hardness does not present too much changes. When the tempering temperature increases from 250 °C, the content of the ε-carbide gradually increases. The tensile strength gradually increases due to the dispersion strengthening of the ε-carbide. However, with further increase of the tempering temperature, the ε-carbide transforms to the cementite, which reduces its dispersion strengthening effect on the martensite matrix. So the tensile strength gradually decreases. The variation tendency of yield strength can be discussed by considering the phase transformation of carbide and the austenite. Firstly, the ε-carbide is coherent with the martensite matrix Refs. [27, 31–33]. The lattice misfit between ε-carbide and martensite matrix is lower 5%, there is significant strain energy associated with this coherent precipitates. When the dislocation moves through the coherency stress field, a strengthening effect generates due to the elastic interaction. James [34] also found that the ε-carbide could effectively improve the strength during tempering. But when the ε-carbide transforms to cementite, this coherent relation will be destroyed, and the coherent strain energy disappears Ref. [35]. The strengthening effect will be weakened. This leads to the decrease of the yield strength. Secondly, the retained austenite will decompose and its amount gradually reduces during tempering. Wang [36] found that the yield-to-tensile ratio gradually decreases with the reduction of retained austenite quantities, which may be another factor for the decrease of the yield strength.

In general, the microhardness has a linear correlation with the tensile strength and the yield strength. However, it is interesting to note that it presents an incomplete linear correlation for LSFed 300M steel. Cahoon et al. [37–39] offered the expressions relating the hardness and tensile strength and yield strength in the form of

$$TS = \left(\frac{HV}{2.9}\right)\left(\frac{n}{0.217}\right)^{n} \quad (1)$$

$$YS = \left(\frac{HV}{3}\right)(0.1)^{n} \quad (2)$$

Where TS and YS are tensile strength and yield strength, respectively, and n is the strain-hardening exponent. These expressions show excellent agreement (<2%) in calculating the tensile properties of a ferritic steel at temperatures up to 400 °C. E.J. Pavlina [40] studied the hardness as well as the yield and tensile strength over 150 steels. He also found that the tensile strength and yield strength show a linear relationship with the hardness. But it can be seen from the hardness-strength data grouped by the microstructure that the correlation for the martensitic microstructures is not good for the tensile strength and the yield strength when the hardness above 500 H V. The microstructure of LSFed 300M steel mainly consists of tempered martensite and a small amount of bainite. The hardness of LSFed 300M steel is about 600–650 H V and its notch sensitivity is high. The combination of the several factors mentioned above result in an incomplete linear correlation between the hardness and the tensile strength and the yield strength.

3.4. Tensile strength and fracture morphology

The SEM photos of tensile fractography of LSFed 300M steel at room temperature with tempering treatment is shown in Fig. 7. It

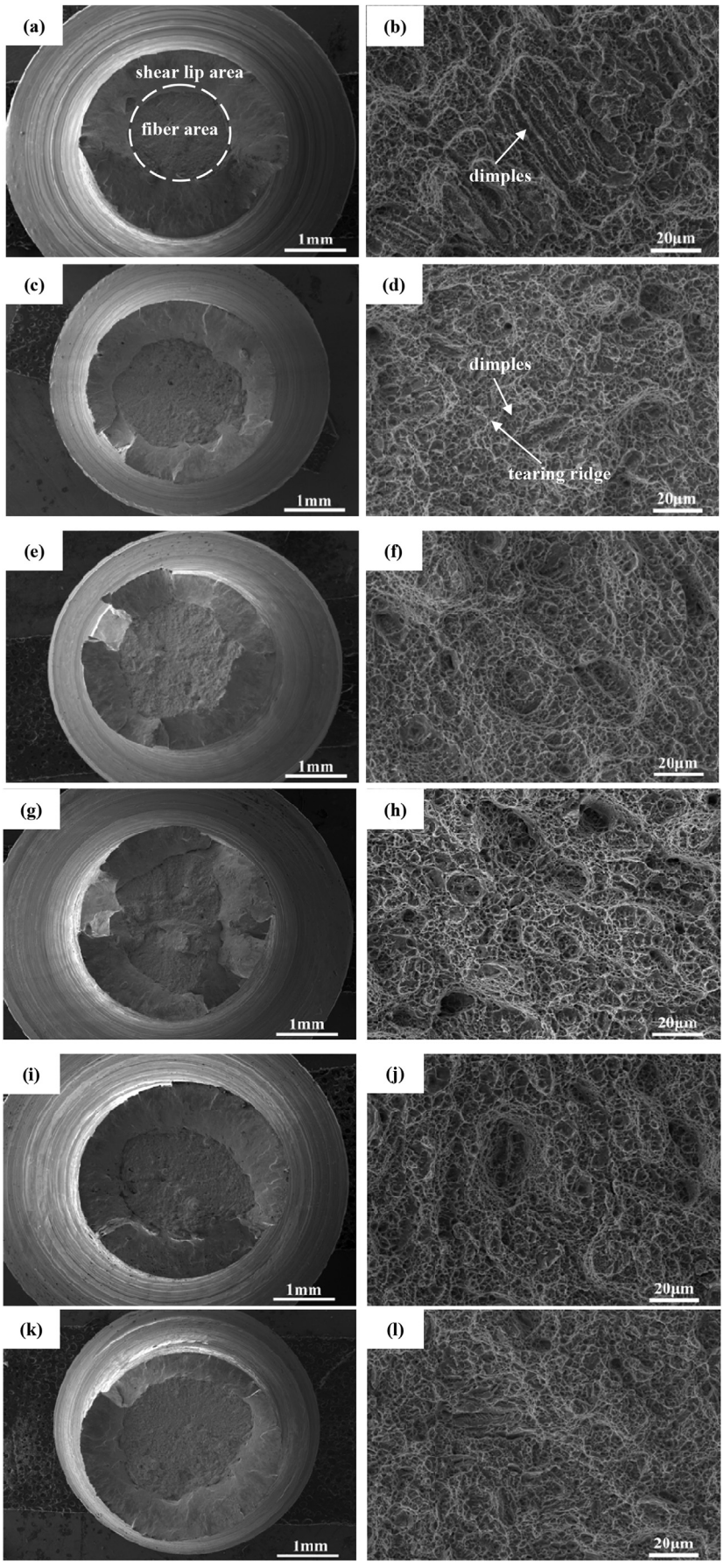

Fig. 7. The fractography of laser solid formed 300M steel with different tempering temperature: (a) (b) 250 °C, (c) (d) 270 °C, (e) (f) 290 °C, (g) (h) 310 °C, (i) (j) 330 °C, (k) (l) 350 °C.

can be seen from macro-morphology that the fracture shows apparent necking deformation (Fig. 7a,c,e,g,i,k). They mainly consist of fiber area and shear lip area (as shown in Fig. 7a). The fracture surfaces of all samples have larger fraction of fiber region, so they present characteristic of ductile fracture. The origin of cracking is in the center of the fracture. It can be seen from micro-morphology that the fracture surface has some dimples aligned along the same direction when the tempering temperature is 250 °C, and there are some big dimples around the outside, as shown in Fig. 7b. Laser solid forming is a non-equilibrium solidification process. The as-deposited microstructure exhibited an epitaxial columnar dendritic growth along the deposition direction. The micro-segregation occurs at the interdentritic. It can be seen from Fig. 7b that the present austenitic treatment is not enough to eliminate this micro-segregation completely, the original solidification structure still remains after oil quenching and tempering treatment. Thus, the microvoids is easy to gather and then form the dimples along the dendrites during tensile test. From the measured result of the relative tensile strength, we can see that the micro-segregation does not seem to have no significant influence on the tensile strength.

With increase of the tempering temperature, the dimples arranged along the columnar crystals disappear and then replaces by the equal-axis dimples (Fig. 7d,f,h,j,l). The exact reason for this is a little unclear and that need further study. There are some obviously tearing ridge around the dimples (Fig. 7d). In addition, some small dimples join together to form a big dimple with the size of 10–20 μm in a certain areas. The force state of microvoids is different during the tensile process. So the microvoids have been torn along the orientation of maximum stress and then form the tearing ridge near the dimples. Therefore, the fracture mode of the samples is ductile fracture.

4. Conclusions

1) The microstructure of quenched and tempered 300M steel mainly consisted of the tempered martensite, bainite and a small amount of retained austenite. When the tempering temperature increased from 250 °C to 350 °C, the size of martensite lath and blocky changed little.
2) With increase of the tempering temperature, the precipitation in the martensite had been transformed from ε-carbide to cementite. In another kind of tempered martensite, ε-carbide was found to be precipitated along specific growth directions, with at least two variants for carbide precipitation.
3) The hardness presented an incomplete linear correlation with the tensile strength and the yield strength for LSFed 300M steel. With increase of the tempering temperature, the hardness gradually decreases and fluctuates in a small range of 600–650 H V. But the tensile strength and yield strength increased first and then decreased. The tensile strength reaches the maximum (1966 MPa) with tempering at 290 °C, and the yield strength reaches the maximum value (1661 MPa) with tempering at 310 °C. The elongation and percentage reduction of area had not obvious changes. The tensile fracture of LSFed 300M steel with tempering treatment presented a ductile fracture pattern.

Acknowledgements

The work was supported by National Natural Science Foundation of China (Nos. 51323008, 51475380, 51501154 and 51271213), the Fundamental Research Funds for the Central Universities (No. 3102015BJ(II)ZS013), the Foundation of State Key Laboratory of Solidification Processing (No. 91-QZ-2014) and the Programme of Introducing Talents of Discipline to Universities, China (No. 08040). China Postdoctoral Science Foundation (NO.2015M572598).

References

[1] Y. Tomita, Development of fracture toughness of ultrahigh strength low alloy steels for aircraft and aerospace applications, Mater. Sci. Technol. 7 (1991) 481–489.
[2] Y. Tomita, Development of fracture toughness of ultrahigh strength, medium carbon, low alloy steels for aerospace applications, Int. Mater. Rev. 45 (2000) 27–37.
[3] Z.Y. Zhao, Interview of academician ZHAO Zhen –ye, Aeroengine 35 (2009) 1–4.
[4] W.D. Huang, X. Lin, J. Chen, Z.X. Liu, Y.M. Li, Laser Solid Forming, Northwestern Polytechnical of University Press, 2007.
[5] L. Costa, R. Vilar, T. Reti, A.M. Deus, Rapid tooling by laser powder deposition: process simulation using finite element analysis, Acta Mater. 53 (2005) 3987–3999.
[6] M.H. Song, X. Lin, G.L. Yang, X.Y. Cui, H.O. Yang, W.D. Huang, Influence of forming atmosphere on the deposition characteristics of 2Cr13 stainless steel during laser solid forming, J. Mater. Process. Technol. 214 (2014) 701–709.
[7] R.S. Amano, P.K. Rohatgi, Laser engineered net shaping process for SAE 4140 low alloy steel, Mater. Sci. Eng. A 528 (2011) 6680–6693.
[8] V.K. Balla, S. Banerjee, S. Bose, A. Bandyopadhyay, Direct laser processing of a tantalum coating on titanium for bone replacement structures, Acta Biomater. 6 (2010) 2329–2334.
[9] X.H. Wu, J. Liang, J.F. Mei, C. Mitchell, P.S. Goodwin, W. Voice, Microstructures of laser-deposited Ti–6Al–4V, Mater. Des. 25 (2004) 137–144.
[10] P. Ganesh, R. Kaul, C.P. Paul, P. Tiwari, S.K. Rai, Fatigue and fracture toughness characteristics of laser rapid manufactured Inconel 625 structures, Mater. Sci. Eng. A 527 (2010) 7490–7497.
[11] C.P. Paul, P. Ganesh, S.K. Mishra, P. Bhargava, J. Negi, A.K. Nath, Investigating laser rapid manufacturing for Inconel-625 components, Opt. Laser Technol. 39 (2007) 800–805.
[12] C. Dong, S.Q. Zhang, A. Li, H.M. Wang, Microstructure of ultrahigh strength steel 300M fabricated by laser melting deposition, Acta Metall. Sin. 44 (2008) 598–602.
[13] F.G. Liu, X. Lin, M.H. Song, H.O. Yang, Y.Y. Zhang, L.L. Wang, W.D. Huang, Microstructure and mechanical properties of laser solid formed 300M steel, J. Alloys Compd. 621 (2015) 35–41.
[14] W.W. Peng, W.D. Zeng, C. Kang, Z.Q. Jia, Effect of heat treatment on microstructure and properties of 300M ultrahigh strength steel, Trans. Mater. Heat. Treat. (2012) 94–98.
[15] W. Zhang, Z.Y. Zhao, Y.S. Feng, B. Ling, The retained austenite in isothermally transformed 40CrNi2Si2MoVA steel, J. Aeronaut. Mater. 15 (1995) 27–34.
[16] J.S. Zhao, L.M. Zhang, A study on the dislocation density in 300M steel, J. Beijing Univ. Aeronaut. Astronaut. 1 (1911) 14–17.
[17] J. Youngblood, M. Raghavan, Correlation of microstructure with mechanical properties of 300M steel, Metall. Trans. A 8 (1977), 1439–1438.
[18] W. Lee, T. Su, Mechanical properties and microstructural features of AISI 4340 high-strength alloy steel under quenched and tempered conditions, J. Mater. Process. Technol. 87 (1999) 198–206.
[19] M.G.H. Wells, Acta Met. 12 (1964) 389–399.
[20] B.W. Zhong, Z.Y. Zhao, The properties of aircraft organic glasses and their temperature rise under high-energy light source, Aeronaut. Mater. 9 (1989) 17–22.
[21] K.H. Jack, Iron Steel Inst. Lond. 169 (1951) 26.
[22] R. Padmanabhan, W.E. Wood, On the occurrence of blocky martensite in 300M steel, Mater. Sci. Eng. A 66 (1984) 1–11.
[23] C. Revilla, B. López, J.M. Rodriguez-Ibabe, Carbide size refinement by controlling the heating rate during induction tempering in a low alloy steel, Mater. Des. 62 (2014) 296–304.
[24] W. Yan, L. Zhu, W. Sha, Y.Y. Shan, K. Yang, Change of tensile behavior of a high-strength low-alloy steel with tempering temperature, Mater. Sci. Eng. A 517 (2009) 369–374.
[25] X.G. Tao, L.Z. Han, J.F. Gu, Effect of tempering on microstructure evolution and mechanical properties of X12CrMoWVNbN10-1-1 steel, Mater. Sci. Eng. A 618 (2014) 189–204.
[26] F. Tariq, N. Naz, R.A. Baloch, A. Ali, Evolution of microstructure and mechanical properties during quenching and tempering of ultrahigh strength 0.3C Si–Mn–Cr–Mo low alloy steel, J. Mater. Sci. 45 (2010) 1695–1708.
[27] B.K. Jha, N.S. Mishra, Microstructural evolution during tempering of a multiphase steel containing retained austenite, Mater. Sci. Eng. A 263 (1999) 42–55.
[28] E. Kozeschnik, H.K.D.H. Bhadeshia, Influence of silicon on cementite precipitation in steels, Meas. Sci. Technol. 24 (2008) 343–347.
[29] Z.Y. Xu, Martensitic Transformations and Martensite, The Science Publishing Company, Beijing, 1980, p. 328.
[30] G.R. Speich, Metall. Trans. A 3 (1972) 1043.
[31] A.T.W. Barrow, J.H. Kang, P.E.J. Rivera-Díaz-del-Castillo, The $\varepsilon \rightarrow \eta \rightarrow \theta$ transition in 100Cr6 and its effect on mechanical properties, Acta Mater. 60 (2012) 2805–2815.
[32] Y. Ohmori, I. Tamura, Epsilon carbide precipitation during tempering of plain

carbon martensite, Metall. Trans. A 23 (1992) 2737–2751.
[33] Y. Xiao, W. Li, H.S. Zhao, X.W. Lu, X.J. Jin, Investigation of carbon segregation during low temperature tempering in a medium carbon steel, Mater. Charact. 117 (2016) 84–90.
[34] B.A. James, D.K. Matlock, G. Krauss, in: Interactive Effects of Phosphorus and Tin on Carbide Evolution and Fatigue Propertied of 5160 Steel, 38th Mechanical Processing and Steel Working Conference Proceedings, Vol. XXXIV, Iron and Steel Society, Arrendale, PA, 1997, p. 579.
[35] K. Saeed, K. Mehrdad, Electromagnetic nondestructive evaluation of tempering process in AISI D2 too steel, J. Magn. Magn. Mater. 382 (2015) 359–365.
[36] X.M. Wang, H. Zhao, C.J. Shang, X.L. He, The microstructure and properties of high performance steels with low yield-to-tensile ratio, J. Alloys Compd. 577 (2013) S678–S683.
[37] J.R. Cahoon, W.H. Broughton, A.R. Kutzak, The determination of yield strength from hardness measurements, Metall. Trans. 2 (1971) 1979–2183.
[38] J.R. Cahoon, An improved equation relating hardness to ultimate strength, Metall. Trans. 3 (1972) 3040.
[39] C.Y. Hsu, Correlation of hot-microhardness with elevated-temperature tensile properties low activation ferritic steel, J. Nucl. Mater. 141–143 (1986) 518–522.
[40] E.J. Pavlina, C.J. Van, Tyne, Correlation of yield strength and tensile strength with hardness for steels, J. Mater. Eng. Perform. 17 (2008) 888–893.